Catalyst Stability | Hot Paper

DOI: 10.1002/anie.201407615

Engineering Catalyst Microenvironments for Metal-Catalyzed Hydrogenation of Biologically Derived Platform Chemicals**

*Thomas J. Schwartz, Robert L. Johnson, Javier Cardenas, Adam Okerlund, Nancy A. Da Silva, Klaus Schmidt-Rohr, and James A. Dumesic**

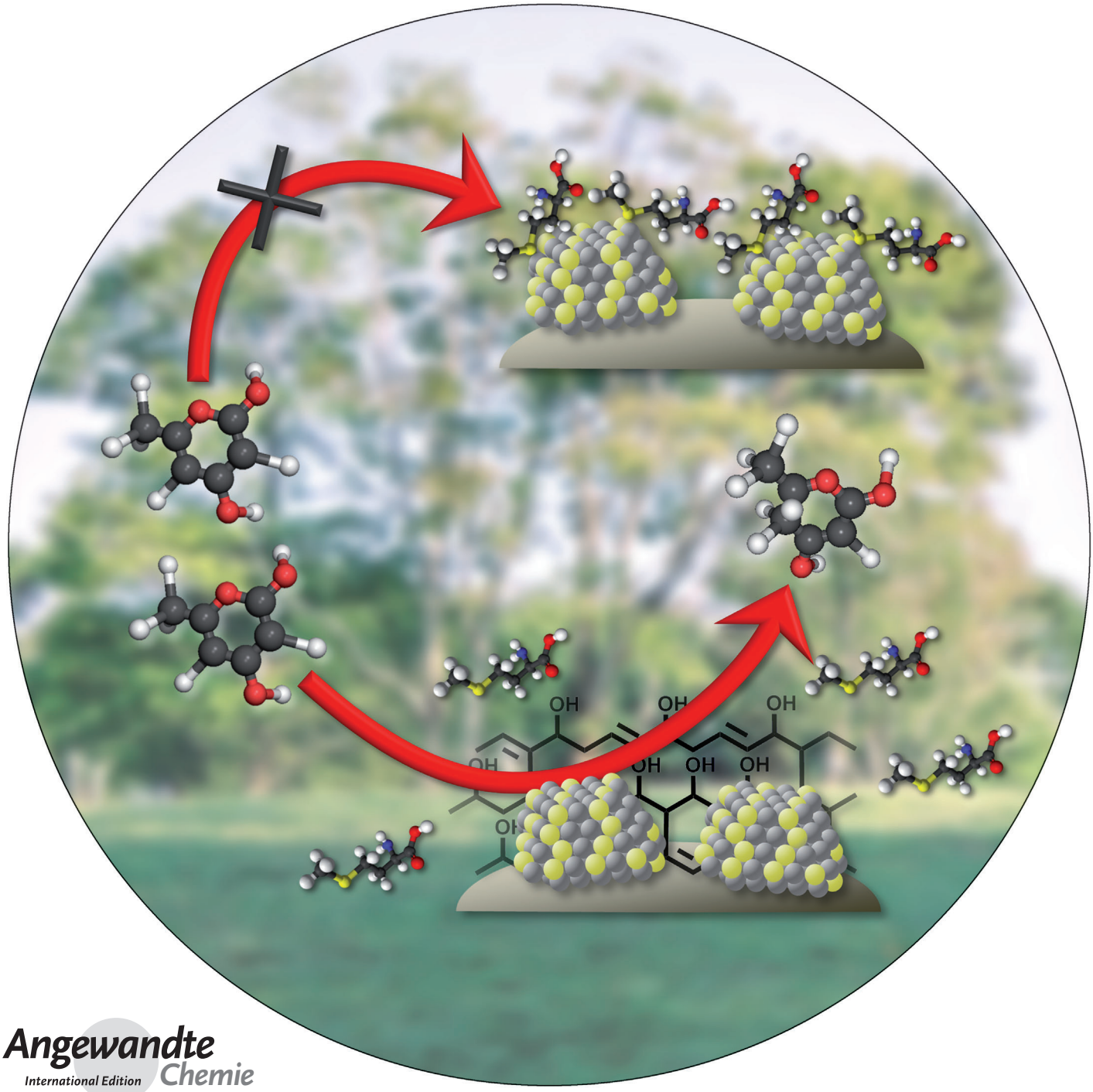

Abstract: *It is shown that microenvironments formed around catalytically active sites mitigate catalyst deactivation by biogenic impurities that are present during the production of biorenewable chemicals from biologically derived species. Palladium and ruthenium catalysts are inhibited by the presence of sulfur-containing amino acids; however, these supported metal catalysts are stabilized by overcoating with poly(vinyl alcohol) (PVA), which creates a microenvironment unfavorable for biogenic impurities. Moreover, deactivation of Pd catalysts by carbon deposition from the decomposition of highly reactive species is suppressed by the formation of bimetallic PdAu nanoparticles. Thus, a PVA-overcoated PdAu catalyst was an order of magnitude more stable than a simple Pd catalyst in the hydrogenation of triacetic acid lactone, which is the first step in the production of biobased sorbic acid. A PVA-overcoated Ru catalyst showed a similar improvement in stability during lactic acid hydrogenation to propylene glycol in the presence of methionine.*

Biomass is an attractive, renewable alternative to petroleum-derived carbon for producing high-value, low-volume products such as chemicals.[1] A recently suggested[2] approach for biomass conversion uses biocatalysis to selectively retain functionality natively present in biomass, leading to highly functionalized platform species. Subsequent chemical catalytic upgrading of these species can then yield drop-in replacements for petroleum.[3] Using this strategy, sorbic acid can be produced from the biologically derived platform molecule triacetic acid lactone (TAL, see Scheme 1).[4] TAL is produced through polyketide biosynthesis, providing an appealing biochemical platform owing to its potential to yield a wide array of highly functionalized species.[2a]

[*] T. J. Schwartz, Prof. J. A. Dumesic
Department of Chemical and Biological Engineering
University of Wisconsin—Madison
Madison, WI 53706 (USA)
E-mail: dumesic@engr.wisc.edu

R. L. Johnson, Prof. K. Schmidt-Rohr
Department of Chemistry, Iowa State University
Ames, IA 50011 (USA)

J. Cardenas, Prof. N. A. Da Silva
Department of Chemical Engineering and Materials Science
University of California, Irvine
Irvine, CA 92697 (USA)

Dr. A. Okerlund
Biorenewables Research Laboratory, Iowa State University
Ames, IA 50011 (USA)

[**] This material is based upon work supported by the National Science Foundation (EEC-0813570). We acknowledge Ana C. Alba-Rubio for collecting STEM images, and acknowledge the use of facilities and instrumentation supported by the University of Wisconsin Materials Research Science and Engineering Center (DMR-1121288). T.J.S. acknowledges support from the National Science Foundation Graduate Research Fellowship Program (DGE-1256259). Any opinions, findings, and conclusions or recommendations expressed in this material are those of the authors and do not necessarily reflect the views of the National Science Foundation.

Supporting information for this article is available on the WWW under http://dx.doi.org/10.1002/anie.201407615.

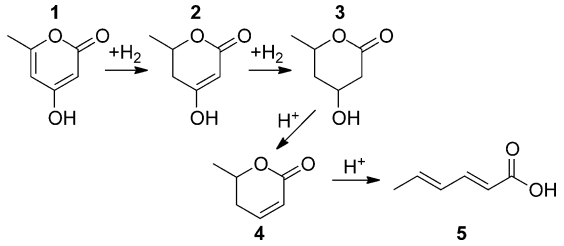

Scheme 1. Conversion of TAL (**1**) into sorbic acid (**5**). This work focuses on the hydrogenation of **1** to 5,6-dihydro-4-hydroxy-6-methyl-2*H*-pyran-2-one (DHHMP, **2**) and 4-hydroxy-6-methyltetrahydro-2-pyrone (HMTHP, **3**). **5** is produced over a solid acid catalyst by dehydrating **3** to parasorbic acid (**4**), which is then ring-opened.[4]

The first step in the conversion of TAL into sorbic acid is the reduction of the unsaturated carbon–carbon bonds in the pyrone ring. However, metal catalysts for hydrogenation are susceptible to deactivation by biogenic impurities in the cell culture medium. Notably, the Ru catalyst used for lactic acid hydrogenation is deactivated through both pore plugging by proteins and competitive adsorption of amino acids.[5] The sulfur-containing amino acids cysteine and methionine (Met) irreversibly poisoned the catalyst at levels as low as 100–150 ppm, indicating a need for complex, expensive separation methods to remove trace amounts of biogenic impurities.

We have previously shown that the surface properties of heterogeneous catalysts can be controlled using an organic polymer to create a microenvironment that surrounds the catalytically active sites.[6] In a similar regard, polymer-encapsulated catalysts have also been developed as a means to immobilize metal-based organic synthesis catalysts, allowing for their recyclability.[7] Herein, we create a microenvironment that surrounds metal nanoparticles by intercalating poly(vinyl alcohol) (PVA) into the pores of the catalyst support. This microenvironment is then used to control which species come into contact with the active sites, thus allowing access of reactants yet mitigating deactivation by suppressing access of biogenic impurities.

The unsaturated carbon–carbon bonds in TAL can be reduced using Pd/C, achieving a 96% yield of HMTHP,[4] a key intermediate for sorbic acid production (see Scheme 1). Quantitative selectivity to DHHMP can also be achieved at 24% conversion using 2% Pd/γ-Al_2O_3. However, as shown in Figure 1a, this catalyst is ineffective for the sustained conversion of TAL because of catalyst deactivation by carbon deposition, an important consideration when upgrading highly functionalized and reactive species such as TAL. The formation of bimetallic PdAu nanoparticles (1:1 atomic ratio) alleviates this deactivation, achieving a DHHMP production rate of 0.9 min^{-1} for at least 50 hours of time-on-stream, while maintaining quantitative selectivity to DHHMP. However, both catalysts were deactivated rapidly in the presence of Met, which was used as a model biogenic impurity (Figure 1b).

The effects on the Pd catalyst of alanine (Ala), tryptophan (Trp), and Met, representative amino acids, were decoupled from catalyst deactivation by TAL by pre-equilibrating the catalyst for 14 hours with a feed containing 0.01 mM of the

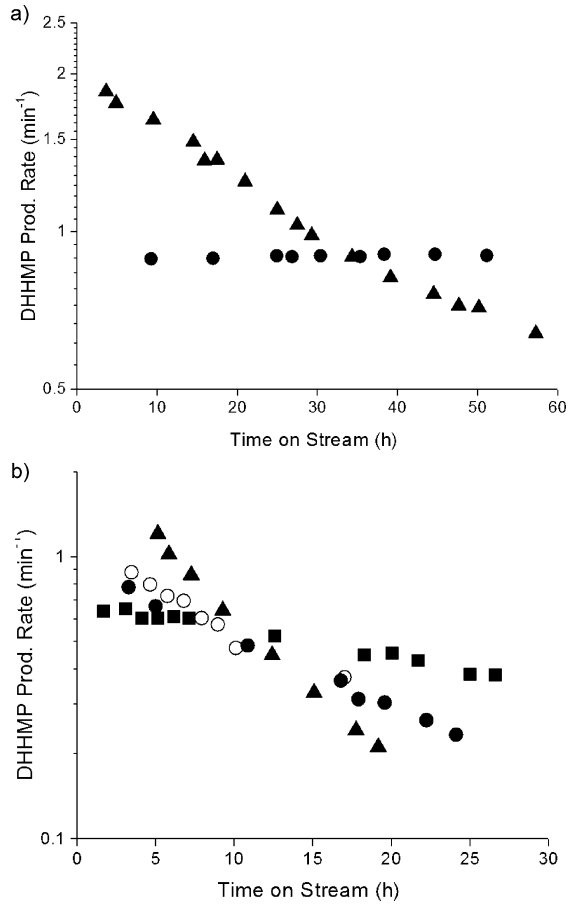

Figure 1. Turnover frequency versus time-on-stream for the hydrogenation of TAL to produce DHHMP over Pd/γ-Al_2O_3 (▲), PdAu/γ-Al_2O_3 (Run 1: ●, Run 2: ○), and PVA/PdAu/γ-Al_2O_3 (■). a) DHHMP production rate for TAL (0.2%) in 1-butanol. b) DHHMP production rate for TAL (0.2%) in 1-butanol with Met (0.01 mM). The initial conversion was between 50–70% in all cases.

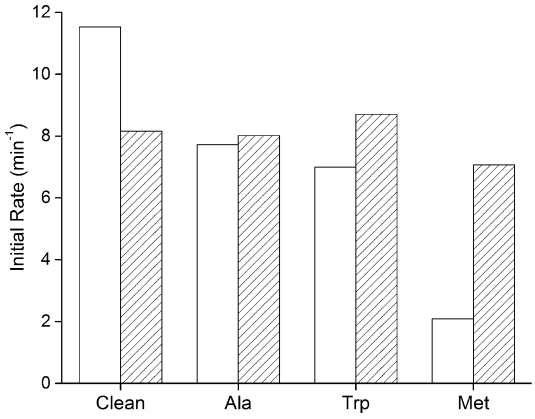

Figure 2. Initial rate of DHHMP production after equilibration for 14 hours in in the presence of three different amino acids (0.01 mM) using Pd/γ-Al_2O_3 (open bars) and PVA/Pd/γ-Al_2O_3 (hashed bars) with TAL (2%) in 1-butanol. The three amino acids are alanine (Ala), tryptophan (Trp), and methionine (Met). The initial conversion was between 30–50% in all cases.

amino acid, after which TAL was added to the feed, and the initial rate of hydrogenation was measured. Low loadings of the amino acids have a strong inhibitory effect on the catalyst (see Figure 2), and this inhibition is governed by the nature of the side chain, in agreement with previous work.[5] Met, with its sulfur group, resulted in 83% deactivation of the Pd catalyst, whereas Trp and Ala, which do not contain sulfur, resulted in 37% and 30% deactivation, respectively. Interestingly, the PdAu catalyst lost only 65% of its activity after nearly 17 hours on stream. Thus, the addition of gold to the catalyst not only prevents deactivation in the presence of TAL, but it also helps to stabilize the catalyst in the presence of sulfur-containing impurities. Importantly, during the first eight hours of time-on-stream over the PdAu catalyst, the decrease in the rate corresponds to a loss of available surface Pd atoms that is equivalent to the amount of Met fed to the reactor. As discussed below, the support does not bind Met when Pd is present, suggesting that Met binds with a 1:1 stoichiometry to the surface Pd in the PdAu catalyst. This observation is consistent with studies of PdAu catalysts used for hydrodesulfurization and hydrogenation, where the presence of gold was shown to inhibit the formation of bulk palladium sulfide, Pd_4S.[8]

Many biogenic impurities, such as amino acids, organic acid byproducts of fermentation, or vitamins, contain polar functional groups, whereas biologically derived platform molecules such as TAL are often less polar. To take advantage of this disparity, we investigated the use of a polymer coating to act as a pseudo-solvent, thus creating a microenvironment that is unfavorable for polar species. The solubility of TAL and amino acids in various solvents was used to guide the selection of the appropriate polymer. In particular, TAL is highly soluble in alcohols (see the Supporting Information, Table S1), whereas amino acids are not,[9] which led to the selection of PVA.

PVA was intercalated into the pores of both the Pd and PdAu catalysts as previously described.[6] Nitrogen physisorption measurements showed minimal changes in porosity following intercalation, although the pore diameter decreased by approximately 1 nm (see Table S2), indicating that the polymer coats the pore walls but does not fill the pores of the support. Moreover, the irreversible CO uptake by the metal nanoparticles decreased following intercalation. Inductively coupled plasma atomic emission spectroscopy of the dissolved catalysts showed that the Pd and Au loadings were both unchanged after overcoating (see Table S2). The surface-weighted average particle size, which was determined by scanning transmission electron microscopy, was unchanged at 3.8 ± 2.9 nm and 3.9 ± 1.3 nm for the parent and overcoated catalysts, respectively. Thus, the decrease in CO uptake is primarily due to site blocking as opposed to sintering or leaching, indicating direct contact between PVA and the metal nanoparticles, as needed to provide a microenvironment in the vicinity of the active sites.

Figure 2 shows that intercalation of the Pd catalyst with PVA decreases the rate of hydrogenation from 11.5 to 8.2 min^{-1}. Importantly, this catalyst shows high activity for TAL hydrogenation after exposure to Met (0.01 mM) for

14 hours. Furthermore, the DHHMP production rate remains essentially unchanged after 14 hours of exposure to Ala (0.01 mM) and Trp as well, demonstrating that the addition of PVA to metal catalysts imparts resistance to inhibitory amounts of polar biogenic impurities. We observed similar effects regardless of polymer chain length, loading, or identity (Table S3). Overcoating the PdAu catalyst with PVA stabilizes the rate of TAL hydrogenation versus time-on-stream in the presence of Met (see Figure 1b), with the first-order deactivation rate constant decreasing from 0.12 h^{-1} using Pd/γ-Al_2O_3 to 0.02 h^{-1} using PVA/PdAu/γ-Al_2O_3.

Based on the improved impurity tolerance of the PVA-overcoated PdAu catalyst, we examined its stability during the hydrogenation of TAL that was produced by engineered *Saccharomyces cerevisiae*, which was expressing a variant of the *Gerbera hybrida* 2-pyrone synthase (2-PS) gene *g2ps1*. The 2PS enzyme uses a single acetyl-CoA starter unit and incorporates two additional malonyl-CoA extenders by iterative decarboxylation–condensation reactions, forming TAL when the triketide intermediate undergoes spontaneous cyclization.[10] Using an *S. cerevisiae* strain engineered for increased precursor availability and an improved 2-PS, we obtained the highest TAL yields described to date, and we have also increased the titer to over 4 g L^{-1}, the highest reported value. Owing to the fact that TAL undergoes decarboxylation at elevated temperature in water,[11] TAL was then recovered from spent culture media prior to hydrogenation (see the Supporting Information, Section 5).

Figure 3 shows that the standard Pd catalyst undergoes rapid deactivation during hydrogenation of recovered and purified TAL, whereas the PVA-overcoated PdAu catalyst is more stable under the same conditions. The first-order deactivation rate constant decreases from 0.31 h^{-1} for Pd to 0.03 h^{-1} for PVA/PdAu. Combined with the observation that the overcoated catalyst is stable in the presence of amino acids, this behavior indicates that the activity loss while upgrading microbially produced TAL is mainly due to the presence of amino acids. Decreasing the amino acid concentration by further purifying the feed using an ion-exchange resin does not result in any improvement in the deactivation rate constant, demonstrating that the overcoated catalyst allows for a simpler TAL recovery process (see the Supporting Information, Section 5).

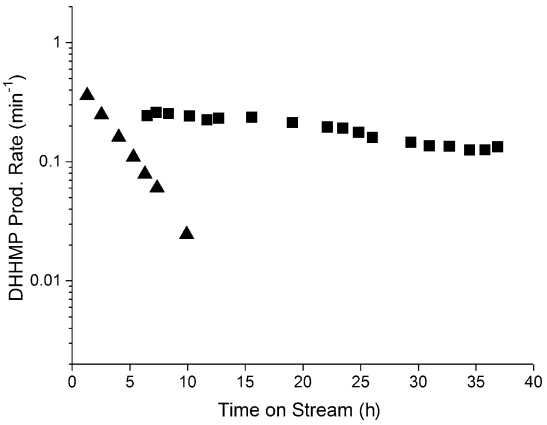

Figure 3. Turnover frequency versus time-on-stream for the hydrogenation of microbially synthesized TAL in 1-hexanol (ca. 0.15%) to produce DHHMP over Pd/γ-Al_2O_3 (▲) and PVA/PdAu/γ-Al_2O_3 (■). The initial conversion was between 50–70% in both cases.

PVA-derived microenvironments can also be used during the hydrogenation of other biologically derived platform species. For example, the supported Ru catalyst that is used for lactic acid (LA) hydrogenation is susceptible to deactivation by Met,[5] and this deactivation was mitigated by overcoating the catalyst with PVA. Overcoating a 5% Ru/γ-Al_2O_3 catalyst increases the propylene glycol (PG) production rate from 0.36 min^{-1} to 0.55 min^{-1} during batch-mode hydrogenation of LA solutions in water (46% w/w; see Table S4). The PG production rate over the Ru catalyst decreased to 0.07 min^{-1} after 14 hours of equilibration with an amount of Met that is equivalent to half the number of surface Ru sites measured by CO chemisorption (Met concentration between 0.8 and 1.2 mM). In contrast, the PVA-overcoated Ru catalyst was more stable after the same treatment, achieving a rate of 0.25 min^{-1}.

To provide insight into the interaction of Met with metal-based hydrogenation catalysts, we treated the Pd catalyst and the γ-Al_2O_3 support with ^{13}C-enriched Met and collected solid-state ^{13}C NMR spectra of these materials. The spectra in Figure 4a show the SCH_3 resonances of neat Met, Met adsorbed on γ-Al_3O_3, and Met adsorbed on Pd/γ-Al_2O_3, which were obtained prior to heating the catalyst in hydrogen. The characteristic 13 ppm signal of Met on γ-A_2O_3 disappears when Pd is present and is replaced by a broader resonance at 19 ppm. Given that the surface area of Pd is much smaller than that of the support, this observation indicates preferential binding of Met to Pd. The large shift in resonance position indicates that the binding involves the SCH_3 group, likely owing to strong S–Pd interactions. Spectra that were obtained after subjecting the catalysts to the reaction conditions (Figure 4b) show substantial changes, indicating Met decomposition.

NMR spectra of the PVA overcoated Pd catalyst (Figure S2) reveal that the support dehydrates about one third of the PVA to form unsaturated carbon–carbon bonds. Treating both the overcoated and non-overcoated catalysts with ^{13}C-labeled Met (0.5 mM) under the reaction conditions and then recording NMR spectra reveals a substantial decrease in the intensity of the Met signal on the overcoated catalyst, demonstrating that Met adsorption is inhibited by the PVA-derived microenvironment (Figure 4b and c). Taken together with the overcoating-induced changes in the support pore diameter and the metal surface area, these observations suggest that the PVA-derived microenvironment imitates a "solid solvent" into which species must partition, analogous to liquid–liquid partitioning. Dehydration of the PVA further suggests that this "solid solvent" is similar to a mixture of nonpolar and polar organic solvents, further decreasing the effective partition coefficient of amino acids and explaining the observed stability of the overcoated catalysts. This interpretation also explains the decrease in the DHHMP production rate following PVA overcoating, because the solubility of TAL decreases in nonpolar organic solvents leading to a lower TAL concentration in the vicinity of the

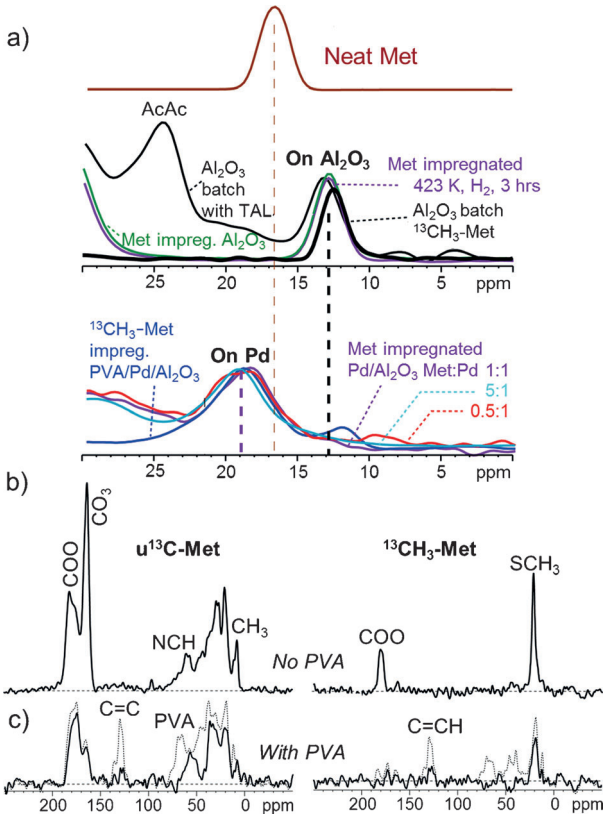

Figure 4. a) ^{13}C NMR resonances from the SCH_3 group of neat Met (top), Met bound to γ-Al_2O_3 (middle), and Met bound to Pd/γ-Al_2O_3 (bottom). b) ^{13}C NMR spectra of Met on Pd/γ-Al_2O_3. c) ^{13}C NMR spectra of Met on PVA/Pd/γ-Al_2O_3. The dashed lines in (c) are the unmodified spectra, and the solid lines correspond to the spectra obtained after subtraction of the PVA background. The spectra in (b) and (c) were obtained using uniformly ^{13}C-enriched methionine (u^{13}C-Met) and methionine with a ^{13}C label on the SCH_3 (^{13}C-Met).

metal nanoparticles. The observed increase in the rate of LA hydrogenation using the PVA-overcoated Ru catalyst can be explained in the same way. In particular, it has been shown that LA is the most abundant surface intermediate on Ru catalysts during LA hydrogenation.[12] As the solubility of LA is decreased in the PVA-derived microenvironment, the decreased local concentration of LA leads to a greater fraction of sites available for reaction and the observed increase in reaction rate.

We have shown that a PVA-overcoated PdAu catalyst is stable for the hydrogenation of TAL, a highly functionalized and highly reactive species, in the presence of biogenic impurities. This catalyst also shows improved stability in the hydrogenation of microbially synthesized TAL. Furthermore, we have shown that a PVA-overcoated Ru catalyst mitigates catalyst deactivation during the hydrogenation of LA in the presence of Met. Accordingly, this work demonstrates that successful coupling of heterogeneous chemical catalysis with biocatalysis is possible in the presence of biogenic impurities, and it provides guidance for developing strategies for upgrading biologically derived platform intermediates.

Received: July 25, 2014
Published online: September 4, 2014

Keywords: biomass · biorenewable chemicals · catalyst stability · hydrogenation · nanocomposites

[1] J. J. Bozell, *Clean Soil Air Water* **2008**, *36*, 641 – 647.
[2] a) B. J. Nikolau, M. Perera, L. Brachova, B. Shanks, *Plant J.* **2008**, *54*, 536 – 545; b) T. J. Schwartz, B. J. O'Neill, B. H. Shanks, J. A. Dumesic, *ACS Catal.* **2014**, *4*, 2060 – 2069; c) B. H. Shanks, *ACS Chem. Biol.* **2007**, *2*, 533 – 535.
[3] a) P. Anbarasan, Z. C. Baer, S. Sreekumar, E. Gross, J. B. Binder, H. W. Blanch, D. S. Clark, F. D. Toste, *Nature* **2012**, *491*, 235 – 239; b) R. M. Lennen, D. J. Braden, R. M. West, J. A. Dumesic, B. F. Pfleger, *Biotechnol. Bioeng.* **2010**, *106*, 193 – 202; c) A. C. Marr, S. Liu, *Trends Biotechnol.* **2011**, *29*, 199 – 204; d) T. Kieboom, *Catal. Renewables* **2007**, 273 – 297; e) O. Pàmies, J.-E. Baeckvall, *Chem. Rev.* **2003**, *103*, 3247 – 3261.
[4] M. Chia, T. J. Schwartz, B. H. Shanks, J. A. Dumesic, *Green Chem.* **2012**, *14*, 1850 – 1854.
[5] Z. Zhang, J. E. Jackson, D. J. Miller, *Bioresour. Technol.* **2008**, *99*, 5873 – 5880.
[6] R. Alamillo, A. J. Crisci, J. M. R. Gallo, S. L. Scott, J. A. Dumesic, *Angew. Chem. Int. Ed.* **2013**, *52*, 10349 – 10351; *Angew. Chem.* **2013**, *125*, 10539 – 10541.
[7] R. Akiyama, S. Kobayashi, *Chem. Rev.* **2009**, *109*, 594 – 642.
[8] a) B. Pawelec, A. M. Venezia, V. La Parola, E. Cano-Serrano, J. M. Campos-Martin, J. L. G. Fierro, *Appl. Surf. Sci.* **2005**, *242*, 380 – 391; b) A. M. Venezia, V. La Parola, G. Deganello, B. Pawelec, J. L. G. Fierro, *J. Catal.* **2003**, *215*, 317 – 325.
[9] K. R. Chalcraft, R. Lee, C. Mills, P. Britz-McKibbin, *Anal. Chem.* **2009**, *81*, 2506 – 2515.
[10] a) J. M. Jez, M. B. Austin, J.-L. Ferrer, M. E. Bowman, J. Schroder, J. P. Noel, *Chem. Biol.* **2000**, *7*, 919 – 930; b) M. B. Austin, J. P. Noel, *Nat. Prod. Rep.* **2003**, *20*, 79 – 110.
[11] M. Chia, M. A. Haider, G. Pollock III, G. A. Kraus, M. Neurock, J. A. Dumesic, *J. Am. Chem. Soc.* **2013**, *135*, 5699 – 5708.
[12] a) Z. Zhang, J. E. Jackson, D. J. Miller, *Ind. Eng. Chem. Res.* **2002**, *41*, 691 – 696; b) Y. Chen, D. J. Miller, J. E. Jackson, *Ind. Eng. Chem. Res.* **2007**, *46*, 3334 – 3340.

